Applied Surface Science 315 (2014) 203–211

Contents lists available at ScienceDirect

Applied Surface Science

journal homepage: www.elsevier.com/locate/apsusc

Modification process optimization, characterization and adsorption property of granular fir-based activated carbon

Congjin Chen[a,b,*], Xin Li[a], Zhangfa Tong[a,b], Yue Li[a], Mingfei Li[c]

[a] School of Chemistry and Chemical Engineering, Guangxi University, Nanning 530004, China
[b] Guangxi Key Laboratory of Petrochemical Resource Processing and Process Intensification Technology, Guangxi University, Nanning 530004, China
[c] Beijing Key Laboratory of Lignocellulosic Chemistry, Beijing Forestry University, Beijing 100083, China

ARTICLE INFO

Article history:
Received 28 April 2014
Received in revised form 16 July 2014
Accepted 19 July 2014
Available online 29 July 2014

Keywords:
Activated carbon modified process
Hydrogen peroxide
Adsorption property
Pore structure characteristics
Surface chemistry

ABSTRACT

Granular fir-based activated carbon (GFAC) was modified with H_2O_2, and orthogonal array experimental design method was used to optimize the process. The properties of the original and modified GFAC were characterized by N_2 adsorption–desorption isotherms, Brunauer–Emmett–Teller (BET) equation, Barett–Joyner–Halenda (BJH) equation, field emission scanning electron microscopy (FESEM), and Fourier transform infrared spectroscopy (FT-IR) analysis, etc. When 10.00 g of GFAC with particle size of 0.25–0.85 mm was modified by 150.0 ml of aqueous H_2O_2 solution, the optimized conditions were found to be as follows: aqueous H_2O_2 solution concentration 1.0 mol·l^{-1}, modification temperature 30.0 °C, modification time 4.0 h. Modified under the optimized conditions, decolonization of caramel, methylene blue adsorption, phenol adsorption and iodine number of the modified GFAC increased by 500.0%, 59.7%, 32.5%, and 15.1%, respectively. The original and optimally modified GFAC exhibited adsorption isotherms of hybrid Type I–IV isotherms with H4 hysteresis. BET surface area, micropore area, total pore volume, micropore volume, and microporosity of the modified GFAC increased by 7.33%, 11.25%, 3.89%, 14.23%, 9.91%, respectively. Whereas the average pore width decreased by 3.16%. In addition, the amount of surface oxygen groups (such as carbonyl or carboxyl) increased in the modified GFAC.

1. Introduction

Granular activated carbon (AC), an artificial carbon material product with a three-dimensional structure, developed pore structure, high specific surface area and good adsorption capacity, mainly composed of carbon (carbon content is 87–97%). It is a safe, non-toxic, and efficient absorbent material which is easy to be produced, utilized, and recycled in large-scale industrialization [1,2]. Its adsorption selectivity to absorbate and the adsorption capacity can be improved by the modification of its surface chemical properties, and pore structure such as pore size distribution [3]. Modified by chemical oxidation/reduction is an effective way to develop special function of AC, reduce the use cost of AC, enlarge its application range and improve its utilization efficiency [3–7].

Oxidation is one of the most conventional modifications used for ACs. It is mainly used to introduce carbon–oxygen surface groups, increase the oxygen-containing acidic groups (such as carboxyl, phenolic hydroxyl, and ester groups, etc.) on the AC surface, and to enhance the surface polarity and hydrophilicity of AC. Oxidation methods involve the utilization of oxidizing gases or oxidizing solutions. The commonly used oxidants are HNO_3 [8–11], O_3 [12,13], $KMnO_4$ [14,15], NaClO [16,17], and H_2O_2 [18,19], and so on. The investigation to examine the effect of H_2O_2 treatment on hydrothermally produced biochar (hydrochar) from peanut hull to remove aqueous heavy metals and the biochar characterization measurements showed that the H_2O_2 modification increased the oxygen-containing functional groups, particularly carboxyl groups, on the hydrochar surfaces [18]. A study on the behavior of CS_2 adsorption on the modified activated carbon (MAC) revealed that the hydrogen peroxide modification led to the increase of basic groups on the surface of AC and CS_2 adsorption capacity [7]. When AC was modified, it was found that both the specific surface area and pore volume increased with the increment of the content of oxygen-containing groups on the surface of MAC [5].

In this paper, granular fir-based activated carbon (GFAC) was modified by the hydrogen peroxide solution, and the effects of aqueous H_2O_2 concentration, modification temperature, and modification time on the adsorption properties of the modified GFAC (MGFAC) were investigated. The pore structure parameters, the surface morphology, and the surface functional groups of GFAC

* Corresponding author. Tel./fax: +86 771 3233718.
E-mail addresses: gxdxccj@163.com, chencongjin@gxu.edu.cn (C. Chen).

http://dx.doi.org/10.1016/j.apsusc.2014.07.111
0169-4332/

before and after modification under optimized conditions were also determined.

2. Experimental

2.1. Materials

GFAC was provided by the Jiangxi activated carbon plant, China, and was selected with particles of 0.25–0.85 mm by sieving. It was washed with deionized water, dried at 105 °C to constant weight, sealed, and stored before use.

Aqueous H_2O_2 concentration (40 wt %) was used as a modification agent. Peracetic acid, glucose, potassium dichromate, anhydrous sodium carbonate, ammonium chloride, methylene blue, phenol, iodine, potassium iodide, sodium thiosulfate, potassium bromide, potassium bromated, copper sulfate, sulfuric acid and other analytical reagents were used as purchased from the Shanghai Sinopharm Chemical Reagent Company Ltd (Shanghai, China). All chemicals were of analytical grade and made in the Spark Chemical Plant, Pudong New Area, Shanghai.

2.2. Orthogonal test methodology for optimizing the modification conditions of GFAC

From the preliminary experimental investigations, H_2O_2 was used as a modification agent to treat AC, in which aqueous H_2O_2 concentration, modification time, and modification temperature were found to be the most influential operational parameters [18,19]. To optimize the modification conditions, an orthogonal test methodology was used [20,21]. An L_{25} (5^6) orthogonal array with six operational parameters was adopted to evaluate the corresponding optimal values. These parameters as well as their range and levels are summarized in Table 1, and the complete design matrixes of the experiments are shown in Table 2.

2.3. Modification of GFAC

In a typical run (Test No. 1 in Table 2), GFAC (10.00 g) with particles of 0.25–0.85 mm were placed in an Erlenmeyer flask, and 150.0 ml of aqueous H_2O_2 at a concentration of 1.0 mol l^{-1} was added. Then the mixture was reacted in a digital water bath oscillator at 30.0 °C and maintained for 1.0 h. After cooling, the resulting mixture was washed with hot distilled water to pH ~ 7.0. MGFAC was filtered, dried at 110 ± 5 °C for 24.0 h, and stored in a tightly closed bottle until further analysis.

2.4. Characterization of GFAC

Iodine number, decolonization of caramel, methylene blue adsorption, and phenol adsorption of GFAC were determined by the test methods of wooden AC GB/T12496.8-1999, GB/T 12496.9–1999, GB/T 12496.10–1999, and GB/T 12496.12–1999 (national standards of China).

The specific surface area and pore structure parameters of GFAC samples was determined by Micromeritics TriStar-3020 adsorption–desorption instrument (American Micromeritics Corp.) and were obtained by nitrogen adsorption–desorption isotherm determined at 77 K. Prior to the test, GFAC was degassed for 2 h at 250 °C under vacuum. The specific surface area, S_{BET}, was determined from the isotherms using the BET equation at a relative pressure of P/P_0 = 0.05–0.35. The total pore (less than 300.00 nm in diameter) volume (V), was defined as the volume of gas nitrogen adsorbed at a relative pressure of $P/P_0 \sim 1$. The micropore volume (V_{micro}), the micropore area (S_{micro}), and the external surface area (S_{exter}) were determined by the t-plot model equation. The adsorption average pore width was calculated using $4V/S_{BET}$; the pore size distribution among 1.70 nm ~ 300.00 nm in diameter was determined using the BJH model equation. The relative growth rate (RGR) of pore structure parameters was calculated according to the following equation:

$$RGR(\%) = \frac{N_{OMGFAC} - N_{OGFAC}}{N_{OGFAC}} \times 100$$

Where N_{OMGFAC} is the value of OMGFAC and N_{OGFAC} is the value of OGFAC.

The morphology of GFAC was examined by U8020 field emission scanning electron microscope (FESEM) (U8020, Japanese Hitachi Corp.) The functional groups on the surface of GFAC samples were identified by Fourier transform infrared spectrometer (FT-IR) (Nicolet 6700, American Nicolet Corp.). OMNIC software was used for the data analysis.

3. Results and discussion

3.1. Orthogonal test

The results of L_{25} (5^6) orthogonal array of the experiments for the modification of GFAC are shown in Table 2. Range analysis of the experimental results of the L_{25} (5^6) orthogonal array is shown in Table 3, and variance analysis of the experimental results of the L_{25} (5^6) orthogonal array is shown in Table 4.

Table 4 Decolorization of caramel is an important index used to evaluate the decolorization ability of AC to pigments in sugar liquid [22]. The composition of the pigments in cane sugar liquid is complex, and it is mainly divided into two categories: nitrogen-containing pigments and no nitrogen-containing pigments. Nitrogen-containing pigments are formed by amino acid, protein decomposition products. No nitrogen-containing pigments are mainly formed by thermal decomposition products of sugar, including some phenols and quinines compounds, and mainly hydroxymethyl furfural compounds. In addition, there are many complexes formed between phenols compounds and iron [23]. The chemical structure of some of these coloring materials is quite complex and difficult to determine in many cases. The most significant colored substances that develop during sugar processing can be classified in three general groups: (a) melanins (b) melanoidins and (c) caramels [24,25]. Because of its molecular size 1.43 × 0.61 × 0.40 nm^3, the methylene blue ($C_{16}H_{18}N_3SCl$) molecule is accessible to the pores with diameters larger than 1.5 nm, methylene blue adsorption is also an important index to evaluate the adsorption capacity of AC to soluble organic macromolecules with diameters less than 1.5 nm [26–28]. Iodine is considered as a molecular probe to assess the adsorption capacity of AC to solutes of molecular size less than 1 nm and iodine number gives information on the surface area contributed by pores larger than 1 nm [28,29]. Phenol, a representative of polyphenols, its longest dimension of the molecular is less than 1.0 nm, is accessible to the pores with diameters larger than 1.0 nm [28]. Decolonization of caramel, methylene blue adsorption, phenol adsorption and iodine number are normally listed as specification parameters for the commercial AC [30]. Therefore, decolonization of caramel (Y_1, %), methylene blue adsorption (Y_2, mg g^{-1}), phenol adsorption (Y_3, mg g^{-1}) and iodine number (Y_4, mg g^{-1}) were determined. The k_n value is the average response value of the operational parameter at the level number n, with the optimum level value when k_n is a maximum. R is defined as the remainder of maximum subtract minimum of the same operational parameter k_n value. The magnitude of R reflects the influence of each factor on the corresponding response. The larger R-value of a corresponding factor, the more significant of the influence of that corresponding factor is. From Table 3, there are significant differences in decolonization of caramel, methylene blue adsorption, phenol adsorption, and

Table 1
Design factors and levels for GFAC modification.

Parameters (Independent variable)	Symbol	Range and levels				
		1	2	3	4	5
Aqueous H_2O_2 concentration (mol l^{-1})	A	1.0	3.0	5.0	7.0	9.0
Modification temperature (°C)	B	30.0	45.0	60.0	75.0	90.0
Modification time (h)	C	1.0	2.0	3.0	4.0	5.0

Table 2
Results of L_{25} (5^6) orthogonal array of the experiments.

No.	*A*	*B*	*C*	Y_1 (%)	Y_2 (mg g^{-1})	Y_3 (mg g^{-1})	Y_4 (mg g^{-1})
1	1.0	30.0	1.0	58.8	165.0	376.1	773.8
2	1.0	45.0	2.0	55.0	142.5	327.2	680.1
3	1.0	60.0	3.0	40.0	127.5	376.1	300.0
4	1.0	75.0	4.0	42.5	126.0	312.6	799.4
5	1.0	90.0	5.0	40.0	127.5	300.4	758.0
6	3.0	30.0	2.0	60.0	150.0	332.1	758.0
7	3.0	45.0	3.0	27.5	135.0	483.6	602.9
8	3.0	60.0	4.0	50.0	127.5	337.0	688.0
9	3.0	75.0	5.0	37.5	100.5	356.6	816.2
10	3.0	90.0	1.0	55.0	135.0	312.6	697.1
11	5.0	30.0	3.0	60.0	172.5	337.0	300.0
12	5.0	45.0	4.0	35.0	133.5	473.8	665.8
13	5.0	60.0	5.0	25.0	97.5	429.8	558.0
14	5.0	75.0	1.0	2.00	105.0	512.8	300.0
15	5.0	90.0	2.0	2.00	78.0	437.2	510.1
16	7.0	30.0	4.0	52.5	141.0	346.8	499.4
17	7.0	45.0	5.0	22.5	120.0	483.6	300.0
18	7.0	60.0	1.0	20.0	93.0	468.9	300.0
19	7.0	75.0	2.0	2.00	78.0	420.1	300.0
20	7.0	90.0	3.0	2.00	60.0	508.0	452.2
21	9.0	30.0	5.0	45.0	105.0	454.2	674.0
22	9.0	45.0	1.0	20.0	91.5	493.3	300.0
23	9.0	60.0	2.0	2.00	60.0	537.3	300.0
24	9.0	75.0	3.0	2.00	60.0	503.1	300.0
25	9.0	90.0	4.0	20.0	115.5	490.9	480.3

Note: *A* represents aqueous H_2O_2 concentration, *B* represents modification temperature (°C), *C* represents modification time (h), Y_1 represents decolorization of caramel (%), Y_2 represents methylene blue adsorption (mg g^{-1}), Y_3 represents phenol adsorption (m^2 g^{-1}) and Y_4 represents iodine number (mg g^{-1}).

Table 3
Range analysis of the experimental results of the L_{25} (5^6) orthogonal array.

	Y_1 (%)			Y_2 (mg g^{-1})			Y_3 (mg g^{-1})			Y_4 (mg g^{-1})		
Levels	*A*	*B*	*C*	*A*	*B*	*C*	*A*	*B*	*C*	*A*	*B*	*C*
k_1	47.2	55.2	31.2	137.8	146.7	117.9	338.5	369.2	432.8	662.2	601.0	474.2
k_2	46.0	32.0	24.2	129.6	124.5	101.7	364.4	452.3	410.8	712.4	509.8	509.6
k_3	24.8	27.4	26.3	117.3	101.1	111.0	438.1	429.8	441.5	466.8	429.2	391.0
k_4	19.8	17.2	40.0	98.40	94.0	128.8	445.4	421.0	392.2	370.3	503.1	626.6
k_5	17.8	23.8	34.0	86.40	103.2	110.1	495.8	409.8	404.9	410.9	579.5	621.2
R	29.4	38.1	15.8	51.40	52.7	27.1	157.3	83.1	49.3	342.1	171.8	235.6

Note: the codes in the table correspond to those in Table 2.

Table 4
Variance analysis of the experimental results of the L_{25} (5^6) orthogonal array.

Index	Parameters	Sums of squares ($\times10^{-3}$)	DOF	Variance($\times10^{-3}$)	*F*	$F_{0.01}$	$F_{0.05}$	Significance
Caramel decolonization capacity	Aqueous H_2O_2 concentration	4.135	4	1.034	7.204	5.41	3.26	**
	Modification temperature	4.221	4	1.055	7.354	5.41	3.26	**
	Modification time	0.7913	4	0.1978	1.379	5.41	3.26	
	Error	1.722	12	0.1435				
Methylene blue adsorption capacity	Aqueous H_2O_2 concentration	9.129	4	2.282	6.427	5.41	3.26	**
	Modification temperature	9.313	4	2.328	6.557	5.41	3.26	**
	Modification time	2.048	4	0.512	1.442	5.41	3.26	
	Error	4.261	12	0.355				
Phenol adsorption capacity	Aqueous H_2O_2 concentration	81.96	4	20.49	13.37	5.41	3.26	**
	Modification temperature	18.78	4	4.695	3.064	5.41	3.26	
	Modification time	8.241	4	2.060	1.344	5.41	3.26	
	Error	18.39	12	1.532				
Iodine number	Aqueous H_2O_2 concentration	471.6	4	117.9	15.16	7.01	3.84	**
	Modification temperature	93.22	4	23.31	2.996	7.01	3.84	
	Modification time	201.7	4	50.42	6.483	7.01	3.84	*
	Error	62.22	8	7.778				

Note: ** represents very significant, * represents significant. DOF represents degree of freedom.

Table 5
The adsorption properties of GFAC before and after modified under the optimal conditions.

Samples	Adsorption properties			
	Y_1 (%)	Y_2 (mg g^{-1})	Y_3 (mg g^{-1})	Y_4 (mg g^{-1})
OGFAC	10.0	108.0	405.4	709.1
OMGFAC	60.0	172.5	537.3	816.2

Note: OGFAC represents original granular fir activated carbon, OMGFAC represents optimally modified granular fir activated carbon. Y_1 represents decolorization of caramel (%), Y_2 represents methylene blue adsorption (mg g^{-1}), Y_3 represents phenol adsorption (m^2 g^{-1}) and Y_4 represents iodine number (mg g^{-1}).

iodine number of the GFAC modified under different conditions, with different factors having different influences on MGFAC. In this experiment, 25 tests were designed. The influence of each factor on the adsorption property of MGAC followed the order, caramel decolonization capacity: $B_1 > A_1 > C_4$, methylene blue adsorption: $B_1 > A_1 > C_4$, phenol adsorption: $A_5 > B_2 > C_3$, and iodine number: $A_2 > C_4 > B_1$. When these factors were optimized, decolonization of caramel, methylene blue adsorption, and iodine number of MGFAC were mainly taken into account. For MGFAC, the following aspects should be considered when optimize the modification conditions: (a) aqueous H_2O_2 concentration had very significant effects on decolorization of caramel, methylene blue adsorption, phenol adsorption and iodine number; (b) the modification temperature had very significant effects on decolorization of caramel, methylene blue adsorption, but had little effects on phenol adsorption and iodine number; and (c) the modification time had significant effects on iodine number, but had little effects on decolorization of caramel, methylene blue adsorption and phenol adsorption. Therefore, A_1, B_1, C_4 was considered to be the optimal condition for modification of GFAC, i.e., aqueous H_2O_2 concentration 1.0 mol l^{-1}, modification temperature 30.0 °C, and modification time 4.0 h.

3.2. GFAC modification under optimal conditions

Table 5 shows the adsorption properties of the original granular fir-based activated carbon (OGFAC) and the activated carbon modified under optimal conditions (OMGFAC). Decolorization of caramel, methylene blue adsorption, phenol adsorption, and iodine number of OMGFAC increased by 500.0%, 59.7%, 32.5% and 15.1%, respectively. This indicated that the adsorption properties of OMGFAC were improved.

3.3. Pore structure of GFAC

The structural heterogeneity of AC has an important influence on the adsorption process, and many methods have been used to characterize this property. Nitrogen adsorption is frequently used at 77 K to probe the porosity and surface area of porous materials because of the relatively small molecular diameter of nitrogen. It has become a standard procedure used to characterize the porosity texture of carbonaceous adsorbents. The adsorption isotherm gives useful information about the pore structure of the adsorbent, such as adsorption heat and physical characteristics. In this study, low-temperature nitrogen adsorption measurement and FESEM methods were used to characterize the pore structure characteristics.

3.3.1. Nitrogen adsorption–desorption isotherms

Fig. 1 illustrates OGFAC and OMGFAC adsorption–desorption isotherms of N_2 at 77 K. The majority of physisorption isotherm may be grouped into six types. Clearly the samples are of hybrid Type I-IV isotherms with H4 hysteresis [31–34]. The initial part of the isotherms is of Type I, indicative of microporosity, hysteresis loop of the isotherms is of Type IV, indicative of mesoporosity. The Type I isotherm is given by microporous solids and is concave to the P/P_0 axis and adsorption amount approaches a limiting value as $P/P_0 \rightarrow 1$. The very steep region at low P/P_0 is due to the filling of very narrow pores and limiting uptake is dependent on the accessible micropore volume rather than on the internal surface area [31–34]. Characteristic features of the Type IV isotherm are its hysteresis loop, which is associated with capillary condensation taking place, and the limiting uptake over a range of high P/P_0 [32]. An absence of hysteresis loop of the isotherms indicated the absence of mesoporosity [35]. This noticeable increase in the quantity adsorbed in desorption branch is attributed to the capillary condensation. The hybrid Type I–IV isotherms with H4 hysteresis is characteristic of solid porous materials having both microporous and mesoporous structures [31–36]. The initial part of hybrid Type I-IV isotherms for carbonaceous adsorbents represents micropore fillings, and hysteresis loop of the isotherms represents the capillary condensation of mesopore. As the authors summarize in Table 6, there are some contributions (small) of microporosity and in a higher proportion mesoporosity as reflected by the PSD.

3.3.2. Characterization of pore structure

The BET surface area (S_{BET}), micropore area (S_{micro}), external surface area (S_{exter}), single point adsorption total pore volume (V), mesopore volume (V_{meso}), micropore volume (V_{micro}), and adsorption average pore width (W_d) ($4V/S_{BET}$) of OGFAC and OMGFAC were obtained by applying the BET equation to N_2 adsorption isotherm at 77 K as shown in Table 6. The relative growth rate (RGR) of pore structure parameters is also listed in Table 6.

Table 6 Pore size distribution is an important property for porous adsorbents. Pore size distribution determines the fraction of the total pore volume accessible to molecules of a given size and shape [34]. According to the IUPAC pore dimension classifications, the pore of a porous absorbent is grouped into micropore ($d < 2$ nm), mesopore ($d = 2$–50 nm) and macropore ($d > 50$ nm). The average adsorption pore width ($4V/S_{BET}$) of OGFAC and OMGFAC was found to be 3.48 nm and 3.37 nm, respectively. The BJH adsorption and desorption cumulative surface areas (S_{BJH}) of pores between 1.70 nm and 300.00 nm in diameter were found to be 341.9 m^2 g^{-1} and 339.6 m^2 g^{-1} in OGFAC, whereas those were 348.5 m^2 g^{-1} and 343.4 m^2 g^{-1} in OMGFAC, respectively. The BJH adsorption and desorption cumulative volumes (V_{BJH}) of pores between 1.70 nm and 300 nm in diameter were found to be 0.5656 cm^3 g^{-1} and 0.5597 cm^3·g^{-1} in OGFAC, whereas those were 0.5663 cm^3 g^{-1} and 0.5585 cm^3 g^{-1} in OMGFAC, respectively. Pore size distribution of OGFAC and OMGFAC calculated using the standard BJH method is displayed in Fig. 2. OGFAC pore size distribution curve (a) and OMGFAC pore size distribution curve (b) showed that the majority of pore volume of OGFAC and OMGFAC were both distributed in pores with an average diameter of 2–50 nm. The BJH adsorption pore size distribution curve (c) indicated that the samples were characterized by a single peak, corresponding to the pore diameter of 11.98 nm and 11.89 nm for OGFAC and OMGFAC. These results confirm that the samples are mainly mesoporous structure with average pore diameter of 6.62 nm and 6.5 nm for OGFAC and OMGFAC, respectively. Desorption branch (curve d) showed again that the samples are characterized by a single peak centered round the pore diameter of 11.92 nm in OGFAC, and 11.90 nm in OMGFAC, and are mainly mesoporous structure with average pore diameter of 6.59 nm and 6.51 nm for OGFAC and OMGFAC, respectively. Fig. 2 shows that most of GFAC pores are in the mesoporous range and Table 6 indicates the microporous structure is simultaneous present. It was found that micropore of OGFAC and OMGFAC showed a smaller contribution to the total pore, since OMGFAC and OGFAC had low microporosities of 27.61% and 25.12%, respectively. Whereas this further proved that OMGFAC formed another micropore when modified with H_2O_2. Thus, both OGFAC and OMGFAC

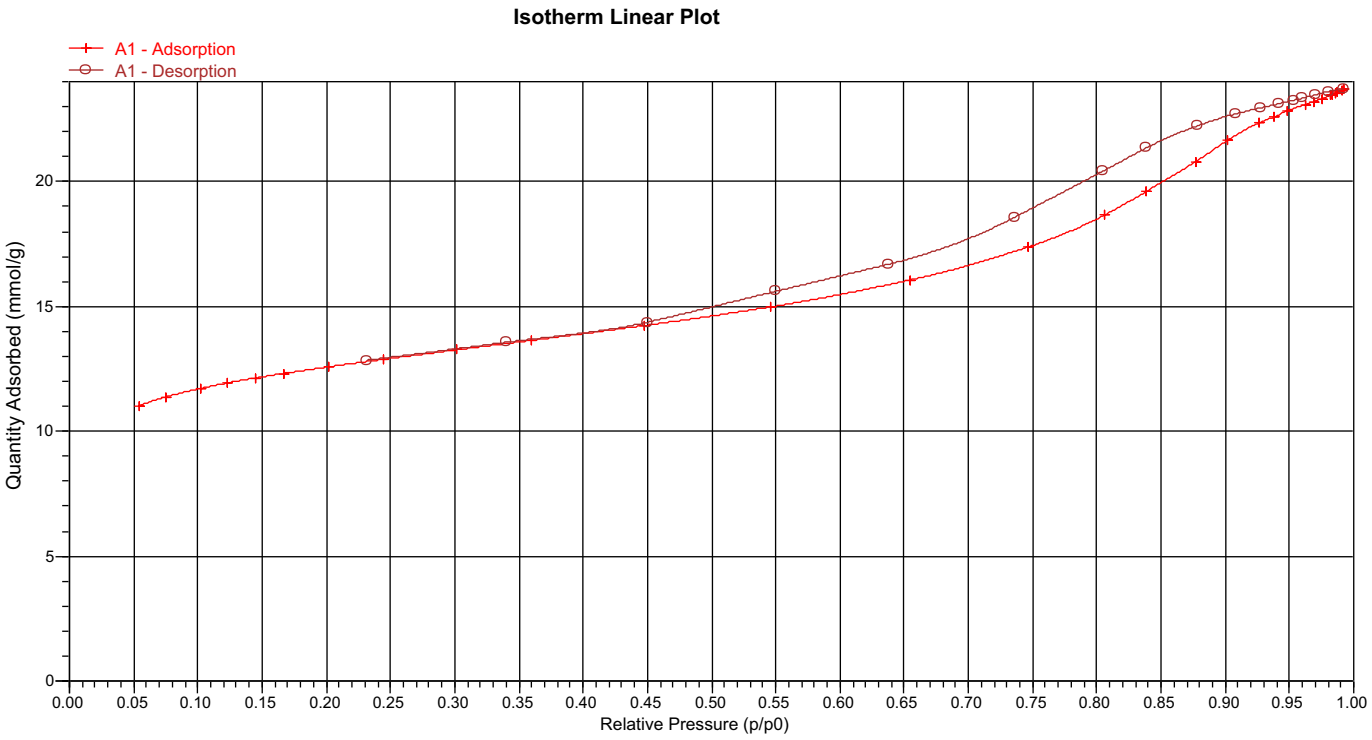

(a) The original granular fir activated carbon (OGFAC)

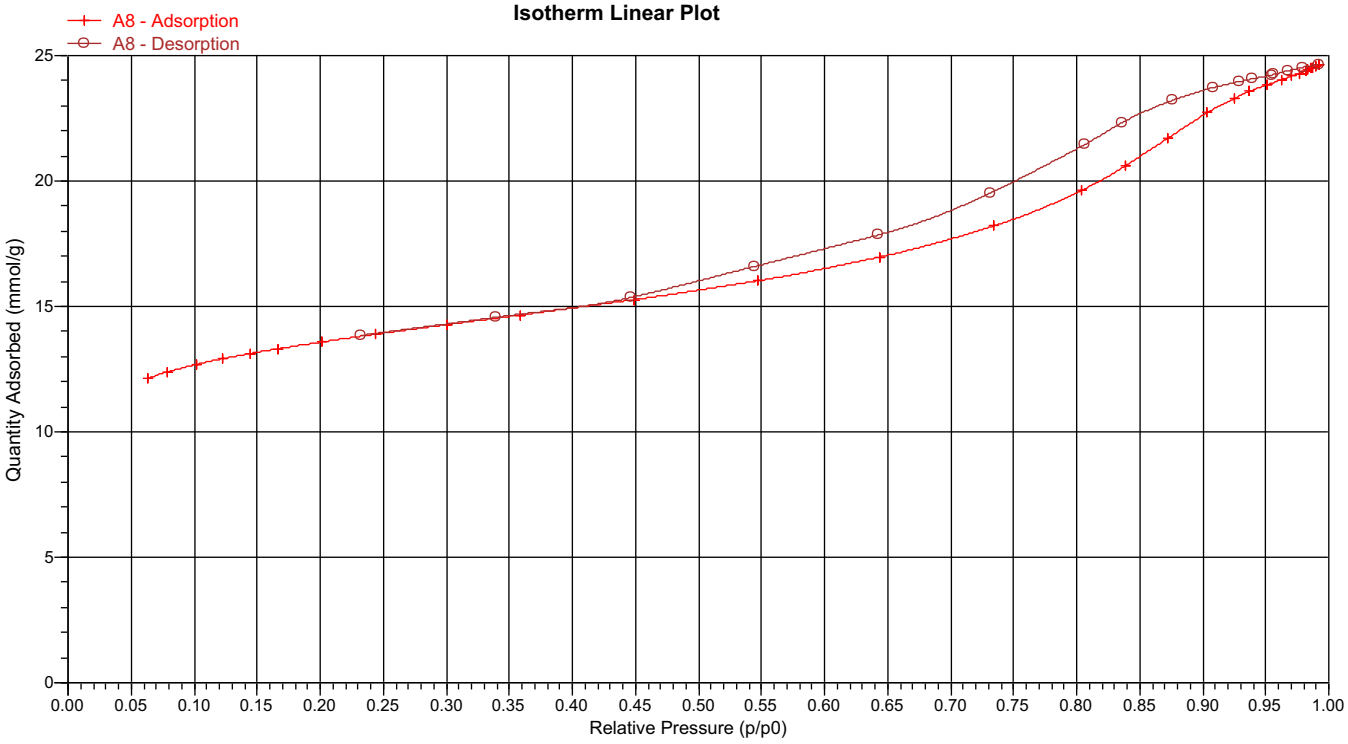

(b) The optimally modified granular fir activated carbon (OMGFAC)

Fig. 1. Adsorption–desorption isotherms of N_2 at 77.35 K on the granular fir activated carbon.

Table 6
Pore structure parameters of OGFAC and OMGFAC.

	S_{BET} ($m^2\ g^{-1}$)	V ($cm^3\ g^{-1}$)	V_{micro} ($cm^3\ g^{-1}$)	V_{meso} ($cm^3 \cdot g^{-1}$)	Microporosity (%)	W_d (nm)	S_{micro} ($m^2\ g^{-1}$)	S_{exter} ($m^2\ g^{-1}$)
OGFAC	944.7	0.8226	0.2066	0.6160	25.12	3.48	534.4	410.3
OMGFAC	1013.9	0.8546	0.2360	0.6187	27.61	3.37	594.5	419.4
RGR (%)	7.34	3.89	14.23	0.44	9.91	−3.16	11.25	2.22

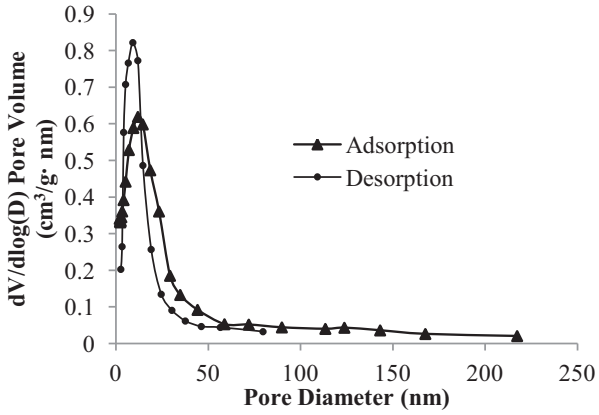

(a) OGFAC pore size distribution curve

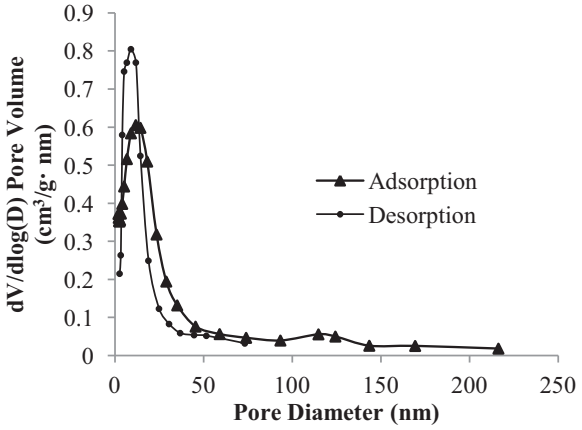

(b) OMGFAC pore size distribution curve

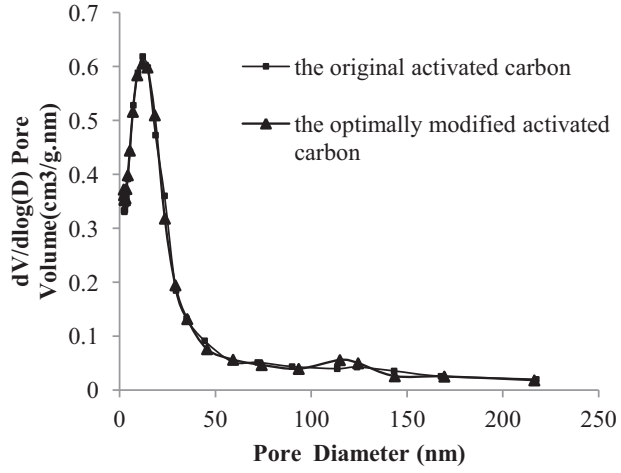

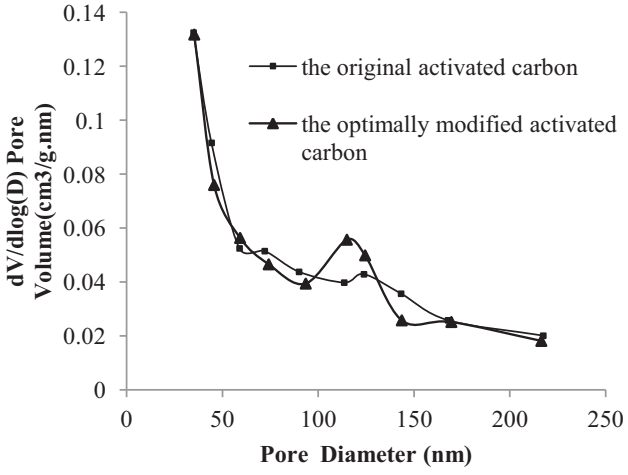

(c) BJH adsorption pore size distribution curve

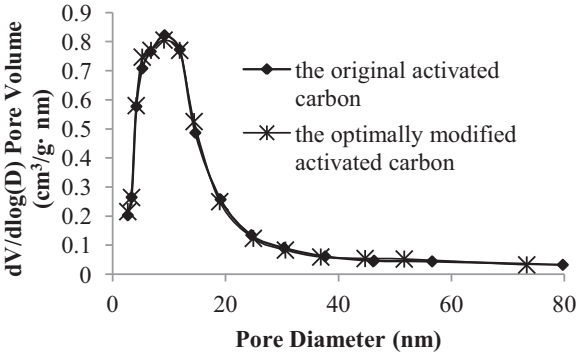

(d) BJH desorption pore size distribution curve

Fig. 2. BJH pore size distribution of OGFAC and OMGFAC.

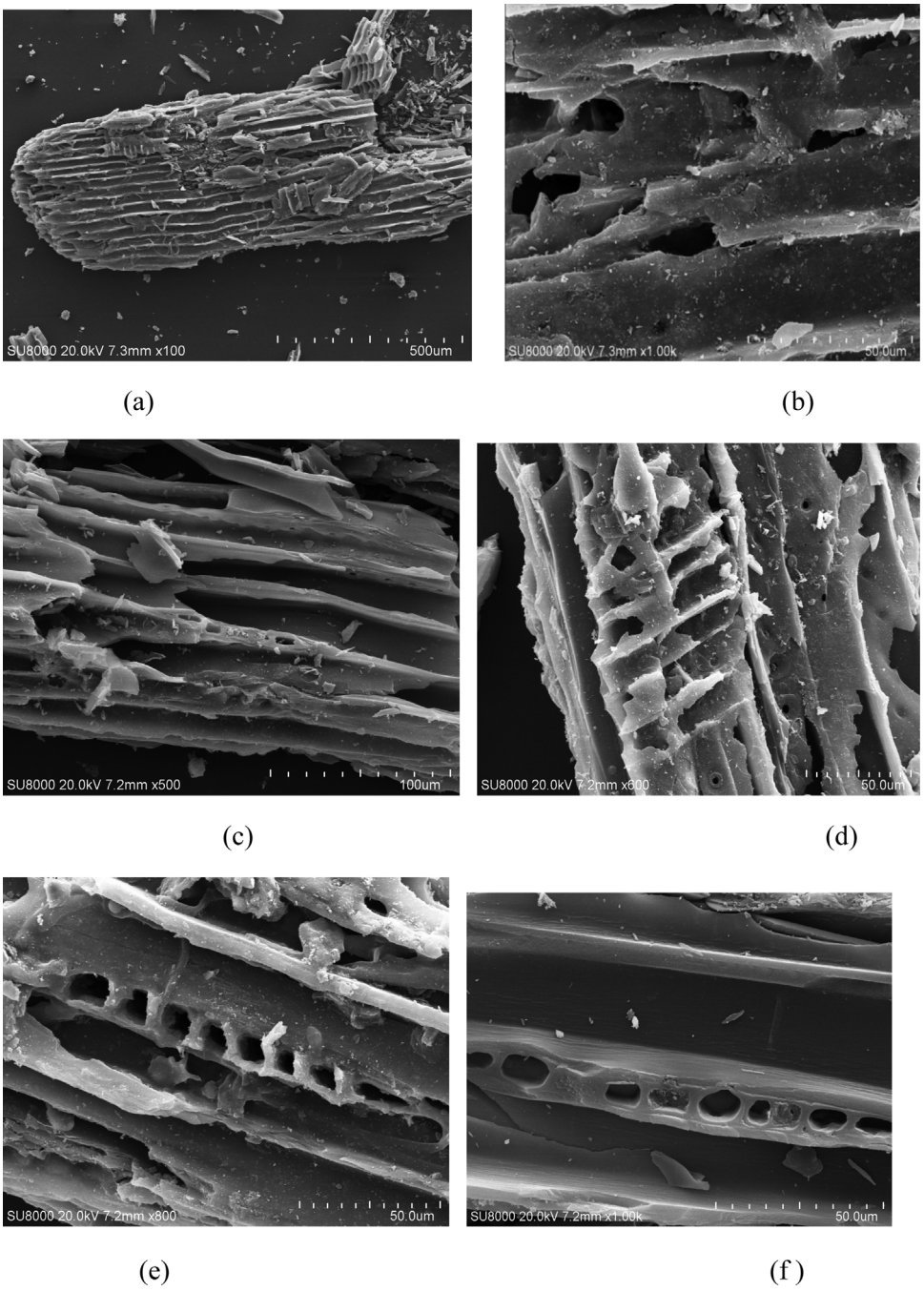

Fig. 3. FESEM images of the original activated and the optimally modified activated carbon.

can be classified into both microporous and mesoporous structures. However, they were both mainly mesoporous.

3.3.3. *Surface morphology*

FESEM was employed to observe the surface physical morphology of the activated carbon. FESEM micrographs of OGFAC (a, b), OMGFAC (c–f) are shown in Fig. 3. It can be seen that the external surfaces of GFAC were full of irregular cavities and pores, and the pore shape was not complete, partially blocked in OGFAC. After modified with hydrogen peroxide, the pore structure exhibited in order, developed porosity, shaped integrity in OMGFAC. After amplified by 600–1000 times, the section of the main pore channel showed numerous tiny pores, and formed a crisscross the channel structure, which increased the specific surface area, total pore volume of OMGFAC. Especially micropore volume, micropore surface area increased, and the average pore diameter of OMGFAC decreased, which make it more conducive to adsorption. As mentioned in Section 3.3.2, GFAC mainly consisted of mesopore together with a small portion of micropore.

3.4. *FTIR of the GFAC*

The FT-IR spectra of OGFAC and OMGFAC are shown in Fig. 4. It can be seen that the overall shapes of the two spectra were very similar. Both spectra show the absorption band at 3444–3420 cm^{-1} due to the O—H stretching vibration. The signal at 2905–2897 cm^{-1} is attributed to C—H (—CH_2, —CH_3, —CH=O) stretching vibrations [37]. The very weak absorptions at 2525 cm^{-1} and 2134 cm^{-1} can

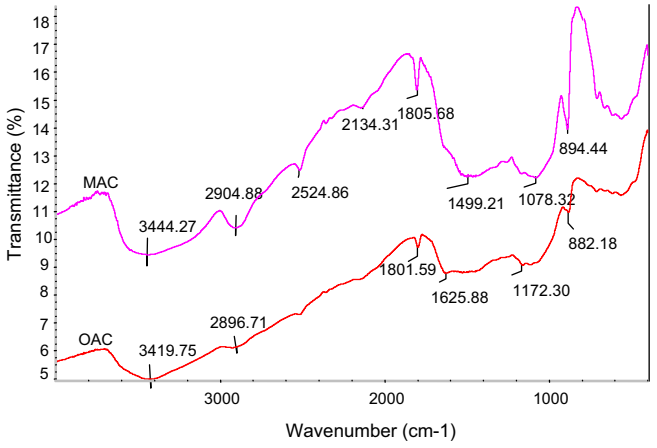

Fig. 4. FTIR spectra of the original activated and the optimally modified activated carbon.

be seen in the FT-IR spectrum of OMGFAC. Such bands have been observed in the earlier IR studies of carbon but the assignments were difficult to be assigned because of the limited number of bands that absorb in these regions. Carbon–oxygen bands have been proposed to give bands at 2525 cm^{-1} and 2134 cm^{-1}, perhaps due to ketene [29]. The bands at 1806–1802 cm^{-1} and 1626 cm^{-1} are attributed to the C═O stretching vibration from carbonyl and carboxyl groups [38,39]. The peak at 1499 cm^{-1} is assigned to the scissoring vibration of the (—CH_2) group, which may overlap with the methyl group asymmetrical bending. It may also be attributed either to the in-plane bending of the H-bonded hydroxyl group, an O—H deformation vibration in carboxyl groups or a C–H bending vibration [37,38]. The peak at 1172 cm^{-1} is associated with phenol (C—O) and O—H bend/stretching vibration [39], and that at 1078 cm^{-1} corresponds to alcoholic C—O stretching vibration [38].The band at 894–882 cm^{-1} is due to (—OC—OH) vibration [40]. The surface functional groups of AC are grouped into three categories: carboxyl-type, carbonyl-type and hydroxyl-type [41]. FT-IR study showed that the amount of surface oxygen complexes such as carbonyl or carboxyl compounds in OMGFAC increased than that in OGFAC.

4. Conclusions

GFAC was effectively modified with H_2O_2. When 10.00 g of GFAC with particle sizes of 0.25–0.85 mm modified by the 150.0 ml of aqueous H_2O_2, the optimized conditions were found to be as follows: aqueous H_2O_2 concentration 1.0 mol l^{-1}, modification temperature 30.0 °C, modification time 4.0 h. Modified under the optimized conditions, the adsorption properties of the MGFAC were improved. Decolorization of caramel, methylene blue adsorption, phenol adsorption, and iodine number of OMGFAC increased by 500%, 59.7%, 32.5% and 15.1%, respectively. OGFAC and OMGFAC both exhibited hybrid Type I-IV isotherms with H4 hysteresis. After modification, BET surface area, micropore area, total pore volume, micropore volume, and microporosity of GFAC increased by 7.33%, 11.25%, 3.89%, 14.23%, 9.91%, respectively. Whereas the average pore width decreased by 3.16%. The amount of surface oxygen-containing groups such as carbonyl or carboxyl also increased.

Acknowledgements

The authors are grateful for the financial support from the National Natural Science Foundation of China (No. 21266002). This project was also supported by Guangxi University and Guangxi Education Department Education Reform in the 21st Century Research Fund of China (No. 2011JGA010), the Dean Project of Guangxi Key Laboratory of Petrochemical Resource Processing and Process Intensification Technology of China (No. 11-C-01-01), the Scientific Research Foundation of Guangxi University (No. XBZ110639) and 2012–2013 “college students’ innovative entrepreneurial training plan” Guangxi autonomous region level Innovation training project (No. 61).

References

[1] J.J. Chen, Y.B. Zhai, H.M. Chen, C.T. Li, G.M. Zeng, D.X. Pang, P. Lu, Effects of pretreatment on the surface chemistry and pore size properties of nitrogen functionalized and alkylated granular activated carbon, App. Surf. Sci. 263 (2012) 247–253.
[2] W.Y. Ding, J.F. Lin, L. Xu, F. Gao, C. Yang, Study of the effects decoloring conditions of powder active carbon on sucrose solution, Acad. Period Farm Prod. Process 166 (2009) 100–102.
[3] Q.S. Liu, T. Zheng, N. Li, P. Wang, G. Abulikemu, Modification of bamboo-based activated carbon using microwave radiation and its effects on the adsorption of methylene blue, App. Surf. Sci. 256 (2010) 3309–3315.
[4] L. Li, P.A. Quinlivan, D.R.U. Knappe, Effects of activated carbon surface chemistry and pore structure on the adsorption of organic contaminants from aqueous solution, Carbon 40 (2002) 2085–2100.
[5] M.S. Shafeeyan, W.M.A.W. Daud, A. Houshmand, A. Arami-Niya, Ammonia modification of activated carbon to enhance carbon dioxide adsorption: effect of pre-oxidation, App. Surf. Sci. 257 (2011) 3936–3942.
[6] X.C. Lu, J.C. Jiang, K. Sun, X.P. Xie, Y.M. Hu, Surface modification, characterization and adsorptive properties of a coconut activated carbon, App. Surf. Sci. 258 (2012) 8247–8252.
[7] S.Y. Tian, H. Mei, Surface modification of activated carbon for CS_2 adsorption and regeneration by microwave heating, Modern Chem. Ind. 32 (2012) 41–45.
[8] P. Vinke, M. van Verbree, A.F. Voskamp, Modification of the surface of gas-active carbon and a chemically activated carbon with HNO_3, Carbon 32 (1994) 675–686.
[9] A.A. El-Hendawy, Influence of HNO_3 oxidation on the structure and adsorptive properties of corncob-based activated carbon, Carbon 41 (2003) 713–722.
[10] K. Tsutsumi, Y. Matsushima, A. Matsuoto, Surface heterogeneity of modified active carbons, Langmuir 9 (1993) 2665–2669.
[11] X.L. Hao, X.W. Zhang, L.C. Lei, Degradation characteristics of toxic contaminant with modified activated carbons in aqueous pulsed discharge plasma process, Carbon 47 (2009) 153–161.
[12] H.L. Chiang, P.C. Chiang, C.P. Huang, Ozonation of activated carbon and its effects on the adsorption of VOCs exemplified by methylethylketone and benzene, Chemosphere 47 (2002) 267–275.
[13] E. Vega, J. Lemus, A. Anfruns, R. Gonzalez-Olmos, J. Palomar, M.J. Martin, Adsorption of volatile sulphur compounds onto modified activated carbons: effect of oxygen functional groups, J. Hazard. Mater. 258 (2013) 77–83.
[14] W. Song, Y. Li, X.H. Guo, J. Li, X.M. Huang, W.J. Shen, Selective surface modification of activated carbon for enhancing the catalytic performance in hydrogen peroxide production by hydroxylamine oxidation, J. Mol. Catal. A: Chem. 328 (2010) 53–59.
[15] A.A.M. Daifullah, S.M. Yakout, S.A. Elreefy, Adsorption of fluoride in aqueous solutions using $KMnO_4$-modified activated carbon derived from steam pyrolysis of rice straw, J. Hazard. Mater. 147 (2007) 633–643.
[16] B. Cagnon, X. Py, A. Guillot, J.P. Joly, R. Berjoan, Pore structure modification of pitch-based activated carbon by NaOCl and air oxidation/pyrolysis cycles, Micropor. Mesopor. Mater. 80 (2005) 183–193.
[17] W.F. Liu, J. Zhang, C. Cheng, G.P. Tian, C.L. Zhang, Ultrasonic-assisted sodium hypochlorite oxidation of activated carbons for enhanced removal of Co(II) from aqueous solutions, Chem. Eng. J. 175 (2011) 24–32.
[18] Y.W. Xue, B. Gao, Y. Yao, M. Inyang, M. Zhang, A.R. Zimmerman, K.S. Ro, Hydrogen peroxide modification enhances the ability of biochar (hydrochar) produced from hydrothermal carbonization of peanut hull to remove aqueous heavy metals: batch and column tests, Chem. Eng. J. 200 (2012) 673–680.
[19] X.L. Song, H.Y. Liu, L. Cheng, Y.X. Qu, Surface modification of coconut-based activated carbon by liquid-phase oxidation and its effects on lead ion adsorption, Desalination 255 (2010) 78–83.
[20] Y.B. Tang, Q. Liu, F.Y. Chen, Preparation and characterization of activated carbon from waste *Ramulus mori*, Chem. Eng. J. 203 (2012) 19–24.
[21] H. Deng, G.L. Zhang, X.L. Xu, G.H. Tao, J.L. Dai, Optimization of preparation of activated carbon from cotton stalk by microwave assisted phosphoric acid-chemical activation, J. Hazard. Mater. 182 (2010) 217–224.
[22] Test methods of wooden activated carbon-Determination of decolorization of caramel. The national standard of the people's Republic of China, GB/T 12496. 9–1999.
[23] G.S. Huang, Y.X. Li, H.P. Mo, Cane sugar manufacturing process technology, second ed., Chinese Light Industry Press, Beijing, 1997.
[24] H.L. Mudoga, H. Yucel, N.S. Kincal, Decolorization of sugar syrups using commercial and sugar beet pulp based activated carbons, Bioresource Technol. 99 (2008) 3528–3533.
[25] M.W. Kearsley, S.Z. Dziedzic, Handbook of starch hydrolysis products and their derivatives, Chapman Hill, London, 1995.

[26] M. Benadjemia, L. Millière, L. Reinert, N. Benderdouche, L. Duclaux, Preparation, characterization and Methylene Blue adsorption of phosphoric acid activated carbons from globe artichoke leaves, Fuel Process.Technol. 92 (2011) 1203–1212.
[27] C. Pelekani, V.L. Snoeyink, Competitive adsorption between atrazine and methylene blue on activated carbon: the importance of pore size distribution, Carbon 38 (2000) 1423–1436.
[28] Z.H. Hu, M.P. Srinivasan, Mesoporous high-surface-area activated carbon, Micropor. Mesopor. Mater. 43 (2001) 267–275.
[29] C.J. Chen, P.C. Zhao, Y.M. Huang, Z.F. Tong, Z.X. Li, Preparation and characterization of activated carbon from eucalyptus sawdust I. Activated by NaOH, J. Inorg. Organomet. Polym. 23 (2013) 1201–1209.
[30] S.Y. Gao, J.B. Zhou, S.L. Zou, C.W. Hu, Q.M. Liu, Ikuo Abe, A study on the relationship between the iodine number, methylene blue adsorption, caramel adsorption and the pore structure of activated carbons, J. Nanjing Forestry Univ. 22 (1998) 23–27.
[31] K.W. Sing, D.H. Everet, R.A.W. Haul, L. Moscou, R.A. Pierotti, J. Rouquero, T. Siemieniewasa, Reporting physisorption data for gas/solid systems with special reference to the determination of surface area and porosity, Pure Appl. Chem. 57 (1985) 603–619.
[32] Z. Ryu, J. Zheng, M. Wang, B. Zhang, Characterization of pore size distributions on carbonaceous adsorbents by DFT, Carbon 37 (1999) 1257–1264.
[33] F. Rouquerol, J. Rouquerol, K.S.W. Sing, Adsorption by Powders and Porous Solids. Principles, Methods and Application, Academic Press, San Diego, 1999.
[34] H. Hadoun, Z. Sadaoui, N. Souami, D. Sahel, I. Toumert, Characterization of mesoporous carbon prepared from date stems by H_3PO_4 chemical activation, App. Surf. Sci. 280 (2013) 1–7.
[35] P. Patnukao, P. Pavasant, Activated carbon from *Eucalyptus camaldulensis* Dehn bark using phosphoric acid activation, Bioresource Technol. 99 (2008) 8540–8543.
[36] P.E.P. Barrett, L.G. Joyner, P.P. Halenda, The determination of pore volume and area distributions in porous substances. I. Computations from nitrogen isotherms, J. Am. Chem. Soc. 73 (1951) 373–380.
[37] B.K. Pradhan, N.K. Sandle, Effect of different oxidizing agent treatments on the surface properties of activated carbons, Carbon 37 (1999) 1323–1332.
[38] C. Moreno-Castilla, M.V. Lopez-Ramon, F. Carrasco-Marin, Changes in surface chemistry of activated carbons by wet oxidation, Carbon 38 (2000) 1995–2001.
[39] S. Shin, J. Jang, S.H. Yoon, I. Mochida, A study on the effect of heat treatment on functional groups of pitch based activated carbon fiber using FTIR, Carbon 35 (1997) 1739–1743.
[40] M.X. Danish, R. Hashim, M.N. Mohamad Ibrahim, O. Sulaiman, Effect of acidic activating agents on surface area and surface functional groups of activated carbons produced from *Acacia mangium* wood, J. Anal. Appl. Pyrol. 104 (2013) 418–425.
[41] K.M. Kim, P.Y. Zhu, N. Li, X.L. Ma, Y.S. Chen, Characterization of oxygen containing functional groups on carbon materials with oxygen K-edge X-ray absorption near edge structure spectroscopy, Carbon 49 (2011) 1745–1751.